Design and Testing of Coils for Pulsed Electromagnetic Forming

S. Golovashchenko[1], N. Bessonov[2], R. Davies[3]

[1] Ford Research & Advanced Engineering, Dearborn, USA
[2] University of Michigan-Dearborn, Dearborn, USA
[3] Pacific Northwest National Laboratory, Richland, Washington, USA

Abstract

Coil design influences the distribution of electromagnetic forces applied to both the blank and the coil. The required energy of the process is usually defined by deformation of the blank. However, the discharge also results in a significant amount of heat being generated and accumulating in the coil. Therefore, EMF process design involves working with three different problems: 1) propagation of an electromagnetic field through the coil-blank system and generation of pulsed electromagnetic pressure in specified areas, 2) high-rate deformation of the blank, and 3) heat accumulation and transfer through the coil with the cooling system. In the current work, propagation of an electromagnetic field in the coil, blank, die and surrounding air was defined using a consistent set of quasi stationary Maxwell equations applying a corresponding set of parameters for each media. Furthermore, a deformation of the blank driven by electromagnetic forces distributed through the volume of the blank was modeled using a solid mechanics equation of motion and the elastic plastic flow theory. During the discharge of capacitors the process was considered to be adiabatic due to the short duration of the pulse, so a heat transfer during the discharge time was neglected. The distribution of electric current density integrated during the discharge process defines the increase of temperature at every element of the coil. The distribution of temperature was calculated as a function of time using the energy conservation law.

Keywords:

Sheet metal forming, Electrical discharge, Tool, Cooling

1 Introduction

Pulsed electromagnetic forming (EMF) uses a coil as tooling, which is employed to generate electromagnetic pressure on the blank during a high-voltage electric discharge of capacitors. Typically, the coil is subjected to the same pressure as the blank. In the

case of a multi-turn coil, additional forces may be generated between the turns of the coil since the clearance between the turns is usually similar to the clearance between the coil and the blank. Typically, the amount of electric energy involved in an EMF process is largely defined by the required deformation of the blank. This electric energy pulse also generates a significant amount of heat after each discharge, which accumulates in the coil over time. In order to implement the EMF technology in high-volume production, an efficient cooling system providing stable temperature of the coil needs to be developed. Therefore, we need to work with three different problems: 1) propagation of electromagnetic field through the coil-blank system and generation of pulsed electromagnetic pressure in specified areas, 2) high-rate deformation of the blank, and 3) heat accumulation and transfer through the coil taking into account the cooling system.

These predictive tools are also a necessary element to design a coil system that would be feasible for high-volume production of automotive panels - specifically of exterior panels with class A surfaces. These predictive numerical models of electromagnetic elastic-plastic forming and heat transfer processes are all important elements for a model that designs a process that works the first time and tolerates high-volume production.

2 Theoretical approach

Propagation of an electromagnetic field within a coil-blank-die-air system can be defined by quasi stationary Maxwell equations:

$$\nabla \times \mathbf{H} = \mathbf{j}, \tag{1}$$

$$\mu_a \frac{\partial \mathbf{H}}{\partial t} = -\nabla \times \mathbf{E}, \tag{2}$$

$$\mathbf{j} = \sigma\left(\mathbf{E} + \mu_a \mathbf{v} \times \mathbf{H}\right), \tag{3}$$

Where $\mathbf{H}$ is magnetic field intensity; $\mathbf{j}$ is current density; $\mathbf{E}$ is electric field intensity; σ is electric conductivity; $\mathbf{v}$ is velocity; μ_a is magnetic permeability of the medium under consideration. For short duration processes we assume $\mu_a = 4\pi\ x\ 10^{-7}$, H/m. In EMF processes the coil and die are almost stationary, while the blank is quickly accelerated; therefore, the equation for magnetic field intensity $\mathbf{H}$ can be transformed in Lagrangian form. Based upon equations (1)-(3), the equation for vector $\mathbf{H}$ can be written as:

$$\mu_a \frac{\partial \mathbf{H}}{\partial t} = -\nabla \times \left(\frac{1}{\sigma} \nabla \times \mathbf{H} - \mu_a \mathbf{v} \times \mathbf{H} \right), \tag{4}$$

or transformed in integral form

$$\mu_a \frac{d}{dt} \int_V \mathbf{H} dV - \mu_a \oint_S \mathbf{v}\mathbf{H} \cdot d\mathbf{s} = \oint_S \frac{1}{\sigma} d\mathbf{s} \times \left(\nabla \times \mathbf{H}\right). \tag{5}$$

Dynamic elastic-plastic deformation of a solid can be defined by the following equation:

$$\rho \frac{\mathrm{d}}{\mathrm{dt}} \int_{\mathrm{V}} \mathbf{v} \mathrm{dV} = \oint_{\mathrm{S}} \sigma \cdot \mathrm{d}\mathbf{s} + \int_{\mathrm{V}} \mathbf{f} \mathrm{dV}\,, \tag{6}$$

where

$$\mathbf{f} = \mathbf{j} \times \mathbf{B} = -\mu_a \mathbf{H} \times \mathbf{j} = -\mu_a \mathbf{H} \times (\nabla \times \mathbf{H})\,, \tag{7}$$

$\sigma = p\mathbf{I} + \mathbf{S}$ is stress tensor; ρ is density; p is pressure; $\mathbf{S}$ is deviator part of stress tensor,

$$\mathrm{p} = \mathrm{K}\left(\frac{\mathrm{V}}{\mathrm{V}_0} - 1 \right), \quad \mathbf{S} = \mathrm{G}\mathbf{B}_{\mathrm{D}}\,, \tag{8}$$

V and V_0 are actual and original volumes respectively; $\mathbf{B}_{\mathrm{D}}$ is the deviator part of the left Cauchy-Green tensor $\mathbf{B}$; $\mathbf{B} = \mathbf{F} \cdot \mathbf{F}^{\mathrm{T}}$; $\mathbf{F} = \mathrm{d}\mathbf{x} / \mathrm{d}\mathbf{X}$ is deformation gradient tensor; $\mathbf{x}$ is the vector of actual location; $\mathbf{X}$ is the vector of original location; K and G are bulk and shear modulus respectively.

The Von Mises yield criterion is used to describe the elastic limit:

$$-J_2(\mathbf{S}) \le \frac{\sigma_y^2}{3}\,, \tag{9}$$

where σ_y is current plastic flow stress (depends on strain and strain rate).

The energy conservation law is employed in the following form:

$$\frac{d}{dt} \int_V c_V T dV = \int_V P dV + \oint_S \lambda \nabla T \cdot d\mathbf{s}\,, \tag{10}$$

where T is temperature; $P = \dfrac{\mathbf{j}^2}{\sigma}$ is power generated in the form of heat while an electric current is running through the coil and blank because of an active resistance of their materials. The System of equations (5)-(10) represents a full formulation of the problem.

The electromagnetic forming machine serving as a generator of pulsed currents can be represented as R-L-C circuit. An electric current running into a coil-blank system as a boundary condition can be defined by the following equations using an explicit integration procedure.

$$\frac{\mathrm{d(LI)}}{\mathrm{dt}} + \mathrm{RI} = \mathrm{U}\,, \tag{11}$$

$$C \frac{dU}{dt} = -I\,, \tag{12}$$

At every time step we solved equations (11) and (12) and, based upon the defined value of current I, calculated its density in the coil $\mathrm{j} = \mathrm{I} / \mathrm{S}$ at the boundary cross-sections

where S is square of the cross-section of the coil. Boundary conditions for $\mathbf{H}$ were calculated based upon the electric current I employing the following equation:

$$\oint_l \mathbf{H} \cdot d\mathbf{l} = I \,. \tag{13}$$

where **l** is a contour around the lead cross-section. Assuming that H is directed tangential to the cross-sections of the incoming and outcoming leads and uniform along their contours, $\mathbf{H}$ can be defined by (13) as

$$\mathrm{H} = \mathrm{I} / \mathrm{L} \,, \tag{14}$$

where L is the perimeter of the lead of incoming or outcoming cross-sections.
In this formulation the propagation of an electromagnetic field in the coil, blank, die, and surrounding air was analyzed using the same set of equations applying a corresponding set of parameters for each media. Since there is a number of metallic parts in close vicinity to the system (coil bandage, die, clamping system, etc.) we believed that an external screen would be an appropriate boundary condition. According to this assumption, the following boundary condition can be applied to the surface of the screen:

$$\mathbf{H} = 0 \,. \tag{15}$$

This system was solved numerically using the finite volume method, based on a non-orthogonal regular Lagrangian mesh which consists of 8 node cells, shown in Figure 1a. Each cell consists of 24 tetrahedrons. An example of tetrahedron "abcd" is shown in Figure 1. Vertex "b" is in the center of the cell's face, while vertex "c" is in the center of the cell. A control volume V is linked to every node of the mesh. According to the described discretization, each cell contributes to the control volume [2], as shown in Figure 1b.

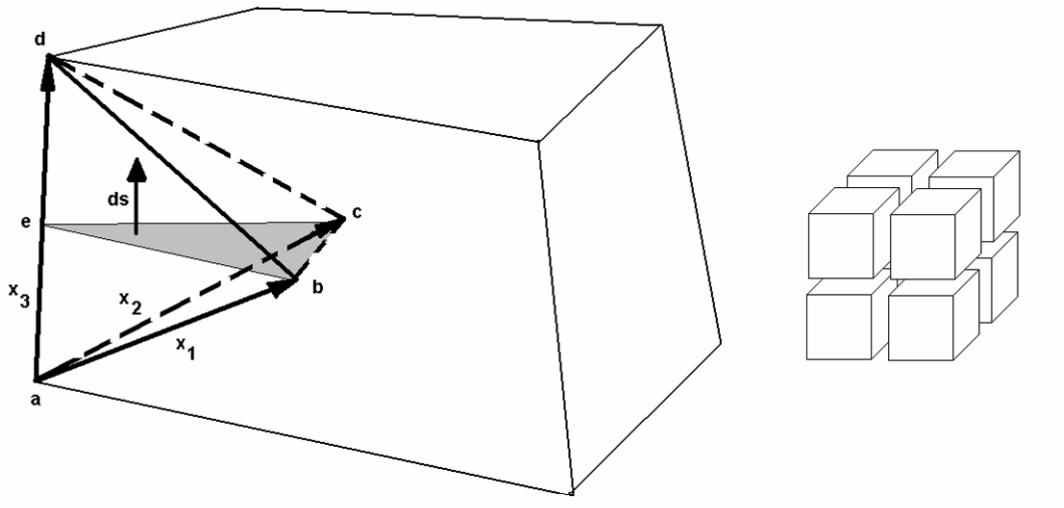

a b

Figure 1: *Numerical mesh in the control volume method*

Equation (5) was solved by integrating the first term in its left side by time:

$$\mu_a V \frac{\mathbf{H}^{n+1} - \mathbf{H}^n}{\Delta t} = \mu_a \oint_S \mathbf{v}\mathbf{H}^{n+1} \cdot d\mathbf{s} + \oint_S \frac{1}{\sigma} d\mathbf{s} \times \left(\nabla \times \mathbf{H}^{n+1}\right), \tag{16}$$

where V is the volume restricted by the surface S; $d\mathbf{s} = \mathbf{n}dS$; $\mathbf{n}$ is the external normal to S. Surface integrals in other terms of (5) are being defined as a sum of surface integrals along the k surfaces of the control volume surrounding this node, as shown in Figure 1.

$$\mu_a \oint_S \mathbf{v}\mathbf{H}^{n+1} \cdot d\mathbf{s} + \oint_S \frac{1}{\sigma} d\mathbf{s} \times \left(\nabla \times \mathbf{H}^{n+1}\right) = \sum_{(k)} \left(\mu_a \mathbf{v}\mathbf{H}^{n+1} \cdot d\mathbf{s} + \frac{1}{\sigma} d\mathbf{s} \times \left(\nabla \times \mathbf{H}^{n+1}\right) \right), \tag{17}$$

The values of $(\nabla \times \mathbf{H})$ and $\mathbf{v}\mathbf{H}$ are considered to be constant for each element of the mesh. The increments of $\mathbf{H}$ in each node of the mesh depend on the values of $\mathbf{H}$ in the elements surrounding the node under consideration. In three-dimensional formulations we have a 27 point pattern. The actual position of the vertices of the tetrahedral element at time t was denoted by $\mathbf{x}_a$, $\mathbf{x}_b$, $\mathbf{x}_c$ and $\mathbf{x}_d$. Let $\mathbf{x}_i$ $(i = 1,2,3)$ be the right-hand set of vectors directed along any three different ribs of the tetrahedron (Fig. 2a). Vector $\mathbf{H}$ was assumed to be a linear function from radius-vector $\mathbf{x}$ in the element:

$$\mathbf{H} = \mathbf{A} \cdot \mathbf{x} + \mathbf{b} \tag{18}$$

$\mathbf{A}$ was defined by the following system

$$\begin{aligned} \mathbf{H}_1 &= \mathbf{A} \cdot \mathbf{x}_1 \\ \mathbf{H}_2 &= \mathbf{A} \cdot \mathbf{x}_2 \\ \mathbf{H}_3 &= \mathbf{A} \cdot \mathbf{x}_3 \end{aligned} \tag{19}$$

Then we obtained

$$\mathbf{A} = \mathbf{H}_i \mathbf{e}_i \cdot \left(\mathbf{x}_m \mathbf{e}_m\right)^{-1}. \tag{20}$$

Using the transformation (20), we defined the approximation of $\nabla \times \mathbf{H}$ in the element

$$\nabla \times \mathbf{H} = \frac{\partial}{\partial \mathbf{x}} \times \left(\mathbf{A} \cdot \mathbf{x} + \mathbf{b}\right) = \frac{\partial}{\partial x_k} \mathbf{e}_k \times \mathbf{H}_i \mathbf{e}_i \cdot \left(\mathbf{x}_m \mathbf{e}_m\right)^{-1} = \mathbf{x}^k \times \mathbf{H}_k, \tag{21}$$

where

$$\mathbf{x}^1 = \frac{\mathbf{x}_2 \times \mathbf{x}_3}{\mathbf{x}_1 \cdot \left(\mathbf{x}_2 \times \mathbf{x}_3\right)}, \qquad \mathbf{x}^2 = \frac{\mathbf{x}_3 \times \mathbf{x}_1}{\mathbf{x}_1 \cdot \left(\mathbf{x}_2 \times \mathbf{x}_3\right)}, \qquad \mathbf{x}^3 = \frac{\mathbf{x}_1 \times \mathbf{x}_2}{\mathbf{x}_1 \cdot \left(\mathbf{x}_2 \times \mathbf{x}_3\right)}. \tag{22}$$

A numerical procedure of integration (6)-(8) simulating the elastic-plastic deformation of the blank was discussed in [1,2]. An explicit integration procedure was considered to be

suitable to simulate a high-rate deformation process. The electromagnetic part of the problem was solved using an implicit integration procedure. In order to reduce computational time for practical three-dimensional problems, the integration step in the EM problem was n times larger than in the elastic-plastic problem. The parameter n was defined for each practical case in order to represent the changes in the distribution of the electromagnetic field appropriately. The clearance between the coil and the blank was expanding due to the acceleration of the blank driven by repelling electromagnetic forces. Therefore, the mentioned clearance was re-meshed periodically.

3 Results of the numerical simulation

The objective of a numerical simulation was to assist the development of the efficient coil for the restrike operation of a preformed aluminum blank. Preliminary experimental results indicated that sometimes electromagnetic pressure is applied in the area where plastic deformation was not expected. Therefore, specific attention was paid to the distribution of electromagnetic pressure and the formation of the blank. Parameters of the discharge were taken from the experimental results produced using a commercial EMF machine and a single turn coil made of aluminum alloy 6061-T6. The maximum energy of the machine was 22.5 kJ with a maximum charging voltage of 15 kV. Two cases were simulated: C=0.0002F and C=0.00025F. Results of the numerical simulation are shown in Figure 2.

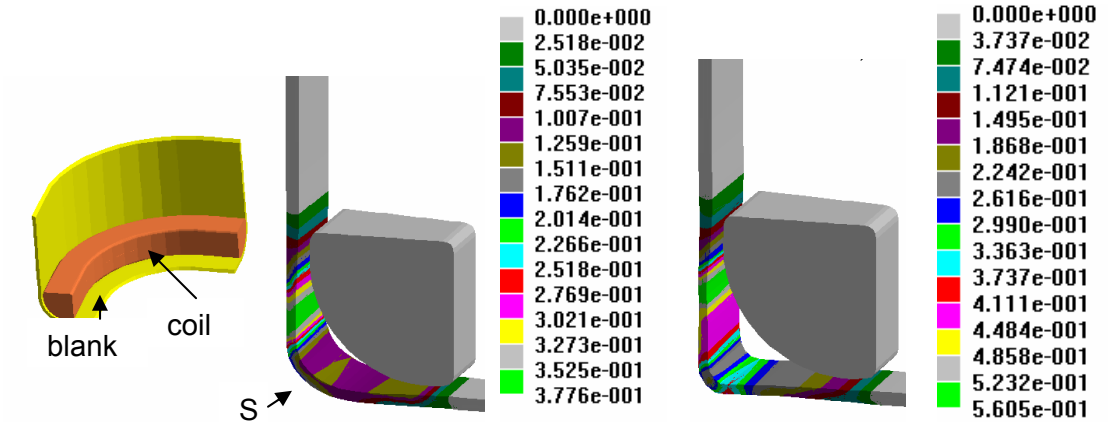

Figure 2: *Results of the numerical simulation of EMF restrike of preformed aluminum blank 1mm thick made of AA6111-T4: a) initial position of the blank and coil; b) position of the blank and distribution of plastic strains in it after the EMF process with the following parameters C=0.0002 F, U=15 kV; c) similar results for the bank of capacitors C=0.00025 F*

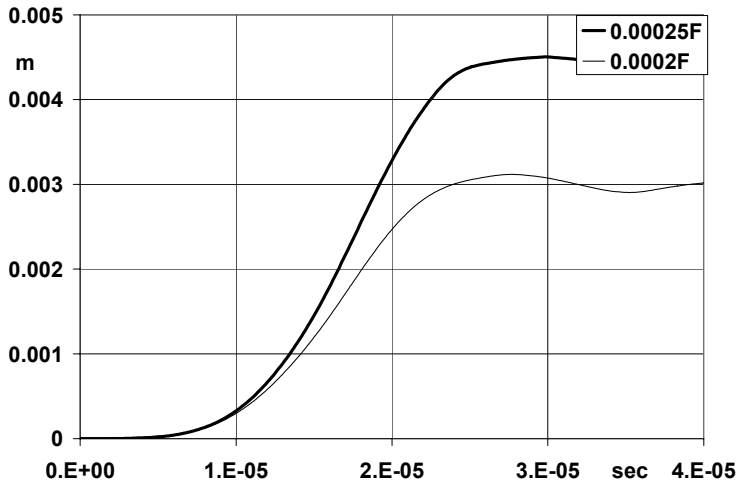

Figure 3: *Radial displacements of the point S vs time for C=0.0002F and C=0.00025F*

Analyzing the strain distribution for two cases, we can conclude that for the case of C=0.00025F maximum plastic strains were at the formability limit. A displacement of the point S of the blank, located on the external surface of the blank, facing the die and belonging to the bisecting line of the angle being formed, is shown in Figure 3.

As it was mentioned before, special attention was paid to the distribution of density of electric currents and pressure applied to the blank. For the single turn coil described above these distributions are shown in Figure 4.

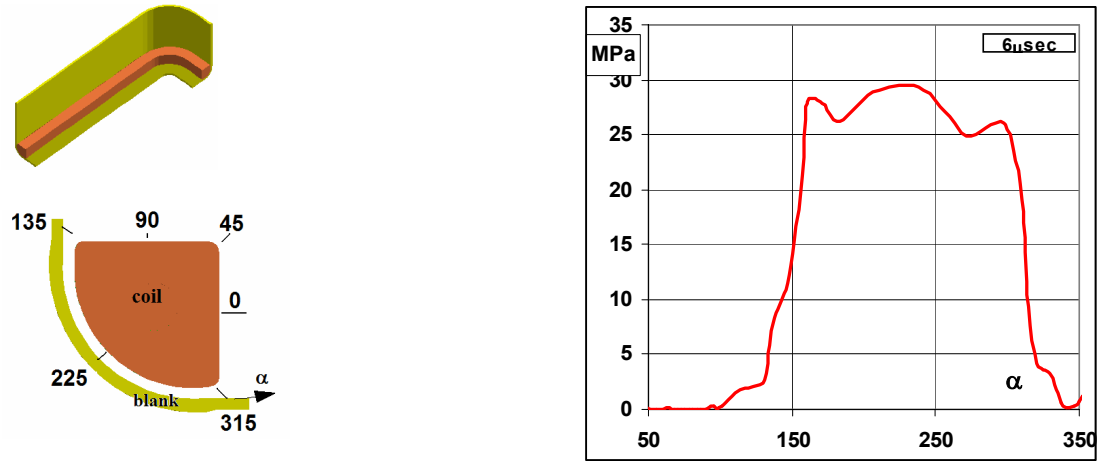

Figure 4: *The coordinate system of a cross-section of the coil (left) and the distribution of EMF pressure at the time moment t=6 μsec after the beginning of the process (right)*

An attempt was made to simulate a composite coil which consists of two parts – a copper layer facing the blank and a steel layer reinforcing the coil against electromagnetic pressure. As a result (Figure 5), the density of electric currents in the area of the cross-section facing the blank can be significantly increased. Even though a composite coil is expected to

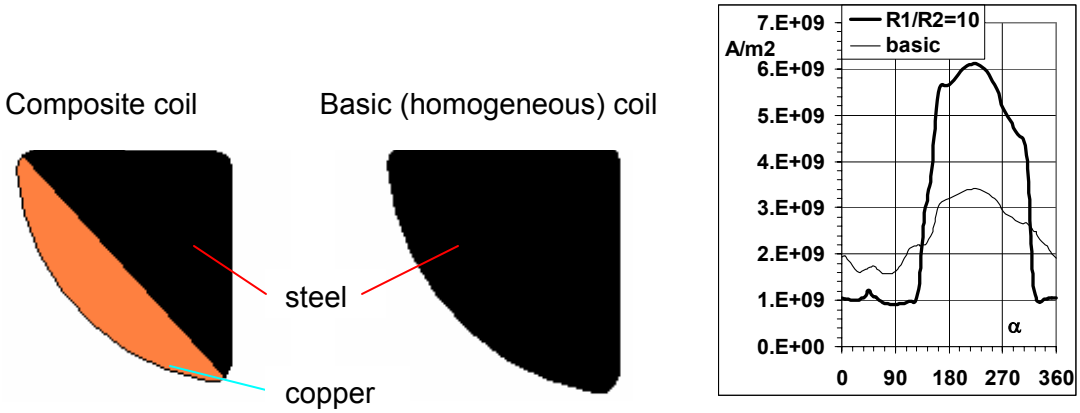

***Figure 5**: Results of the numerical analysis of the composite (copper-steel) coil compared to the basic coil fabricated from steel*

be more expensive due to the necessity of the layers joining, it may provide better efficiency, higher strength, and less heat accumulation compared to the coils made of a homogeneous material. Special attention should also be paid to the accumulation of heat in the coil in high-volume EMF processes. As in well-known induction heating processes, electric currents in EMF processes tend to run within a relatively thin layer due to the "skin" effect. Later, the heat is redistributed due to the material thermal conductivity. After every new discharge of the machine additional heat is being generated in the skin layer. This heat generation process can be considered to be adiabatic. To define the amount of heat, electric current density was integrated over the duration of the process and produced the distribution of heat due to the active resistance of the coil material (Figure 6). Further heat flow and temperature redistribution happens within a much longer period of time between pulses of the EMF machine. In production conditions unloading of the stamped blank and loading of the next blank would take place between two discharges.

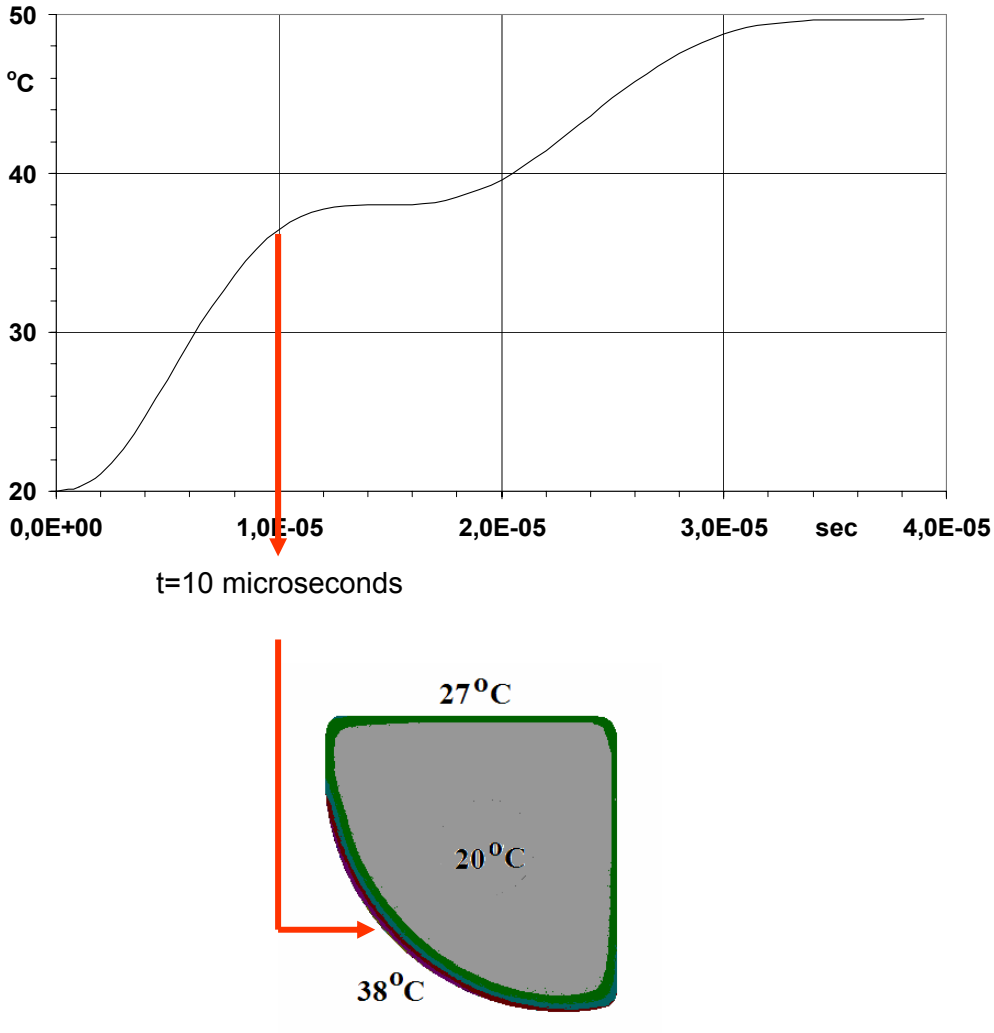

***Figure 6**: Distribution of maximum temperature vs time (upper graph) and distribution of temperature in the coil cross-section (lower graph) during one discharge of the EMF machine*

In order to develop an efficient cooling system of the coil, a numerical model of the heat transfer through the coil was developed. This model took into account the air-cooling system which provided the air flow along the coil surface. The parameter which was expected to drive the cooling process was the velocity of air flow. According to the results of numerical simulation shown in Figure 7, the air flow with the speed of 20 m/sec could accomplish a satisfactory result since it provides a stabilization of the temperature of the coil. Slower air flows of 15 and 10 m/sec provide a stabilization at higher temperatures, which may not be appropriate for the insulation material and may reduce thedurability of the coil.

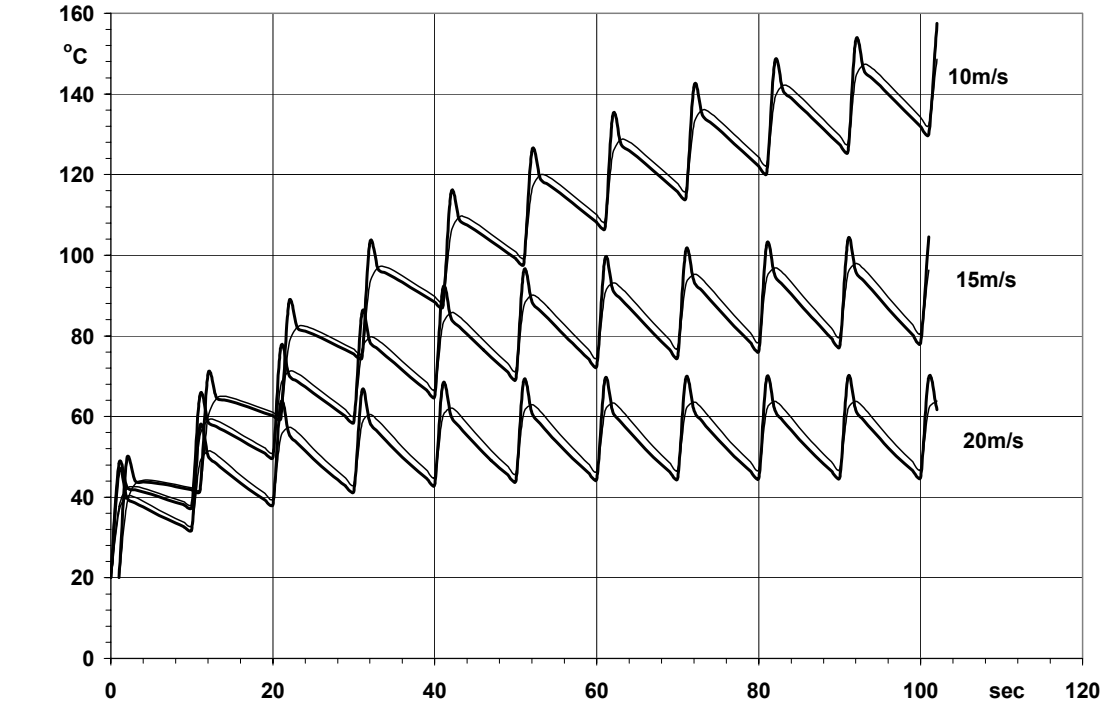

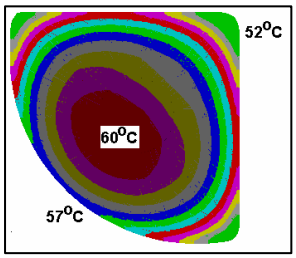

Figure 7: *Maximum (thin lines) and average (thick lines) temperatures of the coil vs. time for production rate of 360 parts/hour with velocity of air flow of 10, 15, and 20 m/sec*

An experimental study of the cooling process was conducted using the flat coil made of steel and micarta insulation plates, illustrated in Figure 8. Air flow was delivered through the slots between the micarta plates in the corners of the coil. The spiral surface was insulated from the blank by a thin plate of insulation material. The air flow was directed between the spiral surface and insulation plate so it would provide cooling of the working surface of the coil where a maximum amount of heat is generated. In this experimental study the energy of the process was specified based upon the energy allowing to form cones made of 1 mm thick aluminum sheet into the die with open round windows 76 mm in diameter, shown in Figure 8. In a durability study the aluminum blank was replaced by an aluminum plate which was clamped to the coil with four bolts, as indicated in Figure 8. An experimental study showed that after 5000 discharges the coil did not have any signs of damage and, therefore, has the potential to be used in high volume production conditions.

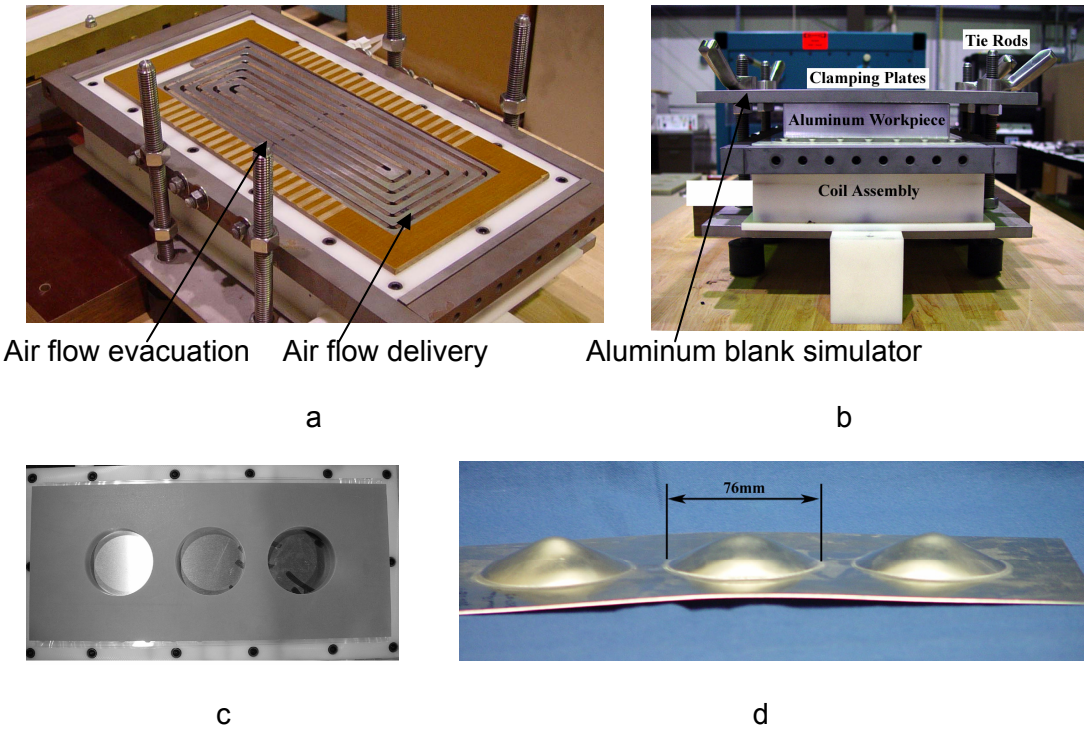

Figure 8: *Experimental fixture employed for an experimental study of coil durability and heat accumulation: a – flat coil with air cooling system; b – assembled fixture for testing coil durability; c - experimental die for estimating the energy of the coil testing procedure; d – formed blank*

4 Conclusions

This work developed numerical models that describe three critical elements of the EMF process: 1) propagation of an electromagnetic field through the coil-blank system and generation of pulsed electromagnetic pressure in specified areas, 2) high-rate deformation of the blank, and 3) heat accumulation and transfer through the coil with an air-cooling system. The process models provide the capability to analyze EMF restrike processes from the perspective of coil design, blank deformation, and cooling systems for the coil.

References

[1] *Bessonov, N.; Golovashchenko S.*: Numerical Simulation of Pulsed Electromagnetic Stamping Processes. Proceedings of the 1st International Conference on High Speed Forming , Dortmund, Germany, 2004, p.83-91.

[2] *Bessonov, N.; Song, D.:* Application of vector calculus to numerical simulation of continuum mechanics problems. Journal of Computational Physics.167/1,1999, p.22-38.